GEOPHYSICAL RESEARCH LETTERS, VOL. 26, NO. 20, PAGES 3133-3136, OCTOBER 15, 1999

# Eddies and the annular modes of climate variability[1]

Varavut Limpasuvan and Dennis L. Hartmann

Department of Atmospheric Sciences, University of Washington, Seattle, Washington

**Abstract.** The dominant modes of month-to-month variation in the troposphere are realistically simulated in a general circulation model whose lower boundary is prescribed with realistic topography and seasonally varying, climatological sea surface temperatures. In both hemispheres, these internal modes describe a nearly zonally symmetric, North-South shifting of the zonal jets as anomalous westerlies vacillate between high (50°-60°) and low (30°-40°) latitudes. The eddy structures evolve with the jets, and the corresponding eddy momentum forcings support the shifts in jet position. Stationary (synoptic) wave variations mainly account for the total eddy forcings in the Northern (Southern) Hemisphere. Pronounced eddy variations occur over the North Atlantic sector.

## 1. Introduction

The month-to-month tropospheric variations in both hemispheres are dominated by a nearly zonally symmetric, North-South movement of momentum and mass across the midlatitudes [*Thompson and Wallace*, 1998 and 1999, hereafter TW]. We refer to these modes of variation as the Northern Annular Mode (NAM) and the Southern Annual Mode (SAM). NAM has also been called the "Arctic Oscillation" by TW, and is related closely to the North Atlantic Oscillation. However, the NAM structure covers a larger extent of the Arctic, and its variability is more closely related to surface air temperature fluctuations over the Eurasian continent. SAM describes zonal flow vacillation in the Southern Hemisphere [e.g. *Hartmann and Lo*, 1998, and references therein]. In this study, we use a realistic numerical simulation to demonstrate the large role of transient and stationary eddy fluxes in the maintenance of these annular modes of variability.

## 2. Model and Analysis

We analyze a 100-year climatological (control) run from the Geophysical Fluid Dynamics Laboratory GCM with rhomboidal 30 horizontal resolution and 14 vertical (sigma) levels (R30L14), extending up to about 10 hPa [*Lau and Nath*, 1990, and references therein]. For this particular run, the sea surface temperatures are given seasonally varying climatological values. Interannual variability is thus absent from the model forcing.

The leading low frequency mode is identified by performing an Empirical Orthogonal Function (EOF) analysis on the monthly anomalies. To produce the anomaly fields, the climatological annual cycle for the 100-year run is first removed from the monthly averaged data. In forming the temporal covariance matrix for the EOF calculation, each grid point in the horizontal data domain is weighted by the square root of the cosine of latitude. The analyzed domains extend poleward from 10° latitude in each hemisphere. Indices of the annular modes are defined as the normalized principal component (PC) time series corresponding to the leading EOF of 1000 hPa geopotential height. Virtually identical indices can be obtained using the sea level pressure fields.

Eddy activity during the extrema of the annular modes is revealed by compositing the eddy fluxes based on the indices of the modes. The high (low) phase composites are averages over months with index values above (below) the +1.5 (-1.5) standard deviation. Synoptic waves are high-pass filtered transients (<10-day period), and stationary waves are zonal asymmetries associated with the monthly composites.

## 3. Structure of the Annular Modes

To a large extent, the month-to-month variation of the entire troposphere can be followed by examining the near surface height field (Z) fluctuation. In both hemispheres, the leading EOF of the 1000 hPa Z shows anomalous low (high) values poleward (equatorward) of about 60° latitude during the high SAM/NAM phase (Fig. 1, top). These modes are well separated from the subsequent modes by the criterion of *North et al.* [1982], and explain 36% and 27% of the total variance in the Southern and Northern Hemisphere, respectively. The structure and amplitude are in good agreement with the observed patterns of TW. However, the NAM height anomalies over the East Siberian Sea are larger than over Greenland in the upper troposphere (e.g. Fig. 1, middle). This behavior differs from observational results based on the National Centers for Environmental Prediction/National Center for Atmospheric Research (NCEP/NCAR) reanalyses [*Limpasuwan and Hartmann*, 1999].

Height patterns at upper levels derived by regressing the anomalous height field onto the SAM/NAM index are highly correlated with the leading Z EOF at those levels. Temporal correlation between the leading Z PC at other levels with the SAM/NAM index are also large (Table 1). As suggested in Table 1, the entire troposphere appears to vacillate about its climatological state in a near zonally symmetric and barotropic manner. This vacillation is most pronounced during the "cold" months of the respective hemisphere (Fig.

[1]Joint Institute for the Study of the Atmosphere and Ocean Contribution Number 673.



Paper number 1999GL010478.
0094-8276/99/1999GL010478$05.00

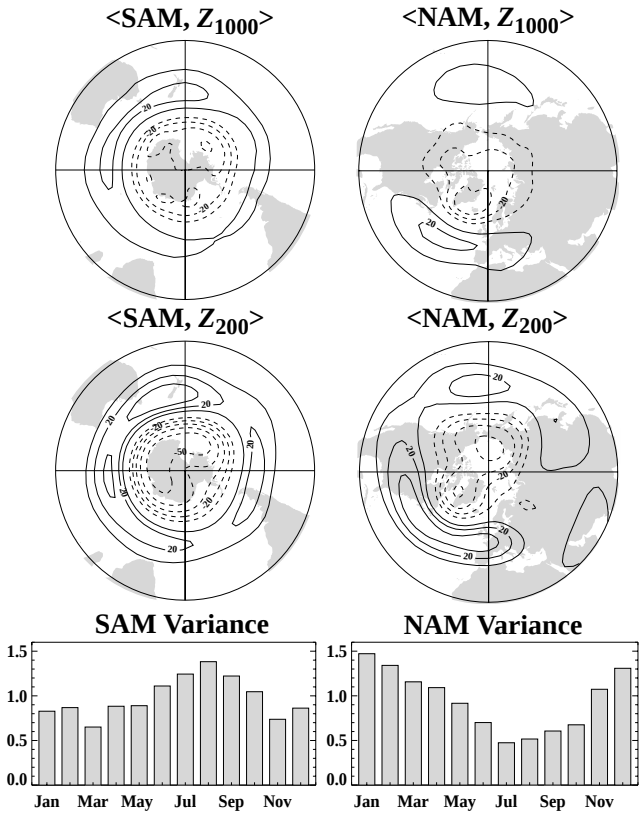


**Figure 1.** (Top) Leading EOF of geopotential height at 1000 hPa ($Z_{1000}$) shown as regression map of $Z_{1000}$ anomalies on the SAM/NAM index. Contour interval is 10 m per standard deviation of the index. Stereographic projection is used. Zero contour is omitted. (Middle) Same as above, except for 200 hPa. (Bottom) The annual cycle of the index variance.

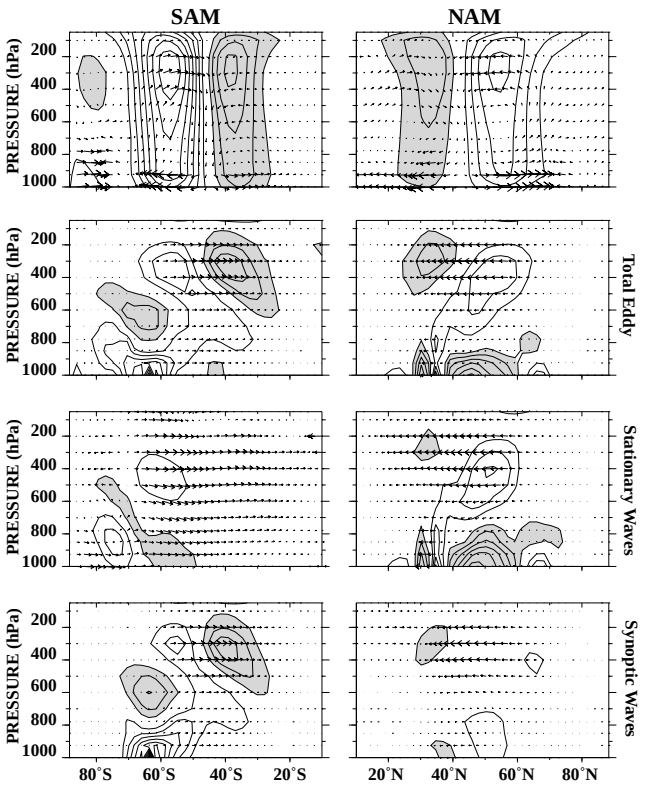


**Figure 2.** (Top) Cross section of the zonal mean zonal wind regressed onto the SAM/NAM index. Contour interval is 0.4 m $s^{-1}$ per standard deviation of the index. Negative values are shaded. The corresponding zonal mean vertical and meridional winds are shown as vectors (magnitude of longest vector is 0.1 m $s^{-1}$). (Others) Composite difference of the EP flux divergence contoured every 0.5 m $s^{-1}$ $day^{-1}$. Easterly acceleration is shaded. Zero contour is omitted. Arrows indicate composite EP vector difference.

1, bottom). The seasonal variation is smaller in the Southern Hemisphere, in agreement with observations.

The zonal jets associated with the annular modes undergo meridional displacement in the midlatitudes at nearly all longitudes. Stronger jets reside at higher latitudes during the high phase, consistent with the contraction of the polar vortex. Cross sections of the anomalous zonal mean zonal wind regressed onto the SAM/NAM index demonstrate shifting of the jets near 30°-50°N or 40°-60°S throughout the troposphere (Fig. 2, top). The associated mean meridional circulation (arrows in Fig. 2, top) describes the modulation of the Ferrel cell. Strongest descending motions are located at the node of the zonal wind anomalies (near 45°) and coincide with a warm region in the analogous regression plot of zonal mean temperature anomalies (not shown). Near the center of strongest zonal wind anomalies, vigorous meridional motions are present near the surface and the tropopause. This suggests that Coriolis acceleration associated with the anomalous surface meridional motion helps sustain the surface wind anomalies while eddy momentum fluxes are important in maintaining the anomalous winds aloft, as demonstrated in a model by *Yu and Hartmann* [1993] and in observations by *Hartmann and Lo* [1998]. Overall, the anomalous mean tropospheric circulation concurs with results of TW. The observed extension of the annular modes into the lower stratosphere is however not obvious in the GFDL model which poorly resolves the

**Table 1.** Relationships of the normalized leading PCs and EOFs for the geopotential height (Z) anomalies at 500, 200, and 100 hPa to the annular modes. Here, <NAM, X>, for example, denotes the spatial pattern derived by regressing Z anomalies at X hPa onto the NAM index.

| | Variance Exp.(%) | | Temporal Correlation w/ | | Spatial Correlation w/ | |
|---|---|---|---|---|---|---|
| EOF/PC | SH | NH | SAM index | NAM index | <SAM, X> | <NAM, X> |
| $Z_{500}$ | 32 | 22 | 0.97 | 0.93 | 0.99 | 0.99 |
| $Z_{200}$ | 29 | 21 | 0.94 | 0.87 | 0.99 | 0.99 |
| $Z_{100}$ | 28 | 24 | 0.88 | 0.67 | 0.99 | 0.95 |

stratospheric circulation. Nonetheless, the observed tropospheric variability is realistically produced in the model.

## 4. Related Eddy Activity and Forcings

Composite difference of the zonal mean momentum eddy forcing (i.e. divergence of the Eliassen-Palm, EP, flux) reveals a westerly-easterly acceleration couplet around the tropopause that nearly coincides with the midlatitude centers of zonal wind anomalies (compare top two panels in Fig. 2). Detailed momentum budget calculations as done by *Hartmann and Lo* [1998] reveal that eddy forcing is mainly due to variations in the eddy momentum fluxes near the tropopause (see also difference EP vectors in Fig. 2, row 2). In NAM (SAM), the total eddy forcings are attributed mainly to stationary (synoptic) waves (see remaining panels in Fig. 2). Mid-frequency transients (10-day<period<60-day) contribute sparingly to the total eddy forcings near the tropopause (not shown). Maintenance of SAM wind anomalies by synoptic waves has also been shown in previous modeling and observational studies of zonal flow vacillation [e.g. *Robinson*, 1991; *Yu and Hartmann*, 1993; *Feldstein and Lee*, 1996; and *Hartmann and Lo*, 1998]. Maintenance of NAM by stationary waves is suggested by *DeWeaver and Nigam* [1999].

Top panels of Fig. 3 summarize the NAM synoptic wave activity as **E** vectors [*Hoskins et al.*, 1983]. The **E** vectors roughly point in the direction of the wave energy propagation, and their divergence approximates the local mean wind acceleration. An equatorward pointing vector indicates poleward eddy momentum flux by the transients. The vertical vector component (shown as contours) reflects poleward eddy heat flux. The synoptic wave activity, localized over the oceanic sectors, fluctuates with the related jet displacement (see contours in Fig. 3, bottom). Wave activity during the high NAM phase is stronger, originates from below at a more poleward position, and tends to propagate more equatorward when the jet is displaced poleward (Fig. 3, top right). Similar contrasts in storm activity between high and low phases are found in the Southern Hemisphere although the eddies are much less localized (not shown).

Bottom panels of Fig. 3 show the NAM stationary waves as $\mathbf{F_s}$ vectors [*Plumb*, 1985] at 300 hPa. The $\mathbf{F_s}$ vector is approximately parallel to the wave energy propagational direction and its zonal mean is equivalent to the EP flux [*James*, 1994]. The stationary wave activity is stronger and propagates more equatorward during the high phase, particularly over the North Atlantic. The associated momentum fluxes conform with the synoptic waves in forcing poleward displacement of the westerlies during the high NAM phase.

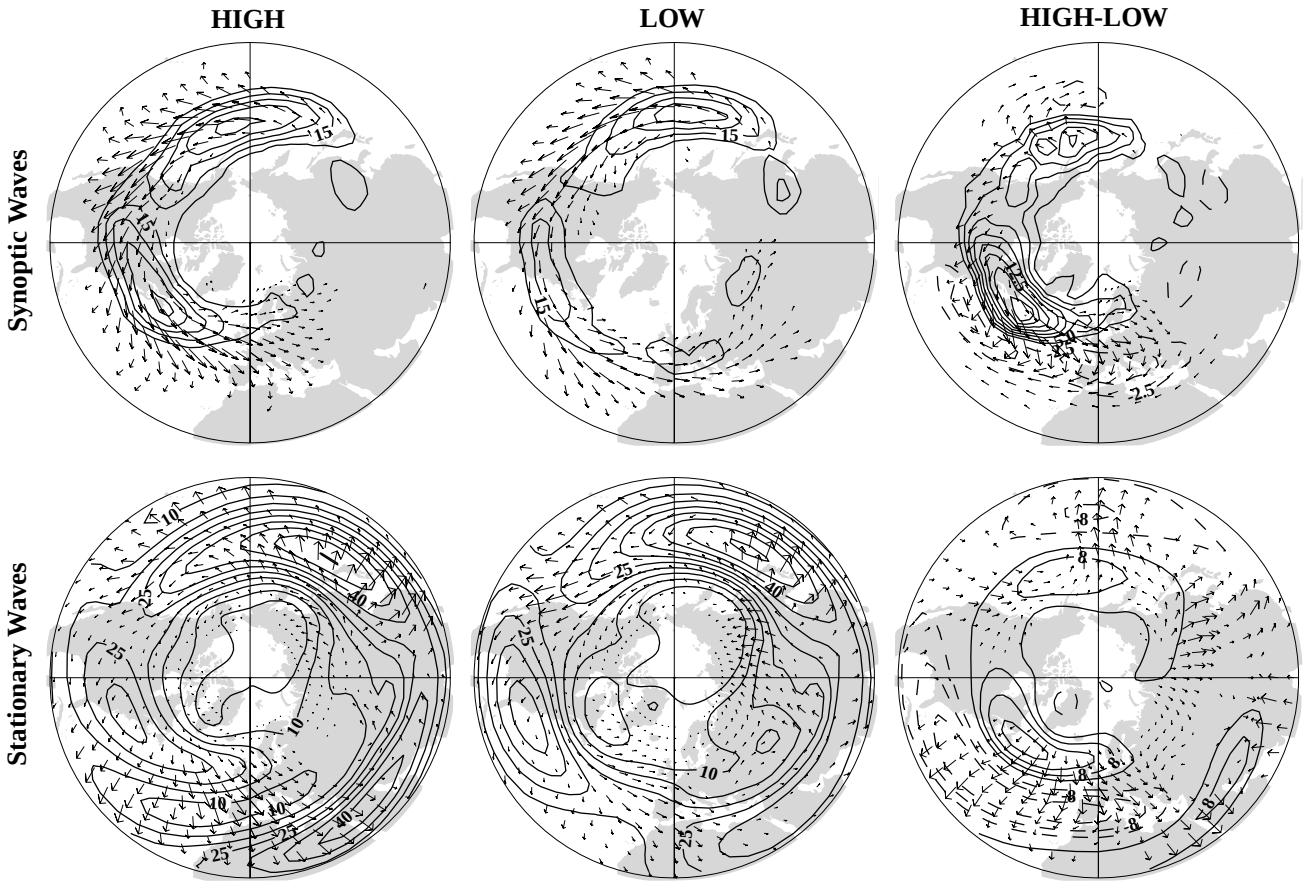


**Figure 3.** (Top) The NAM composite of the synoptic waves (**E** vectors). The horizontal (vertical) vector component is shown as arrows (contours) at 300 (700) hPa. Contour interval is $5.0\times10^{-2}$ m$^2$ s$^{-2}$ (composite) and $2.5\times10^{-2}$ m$^2$ s$^{-2}$ (difference). The longest vector in the composite has a magnitude of 110 m$^2$ s$^{-2}$. (Bottom) The NAM composite of the stationary waves ($\mathbf{F_s}$ vectors) at 300 hPa. Composite zonal winds at 300 hPa are also shown as contours with interval of 5 m s$^{-1}$ (4 m s$^{-1}$, difference). The longest vector in the composite has a magnitude of 22 m$^2$ s$^{-2}$. The vector length in the low composite is scaled relative to the high.

The relationship of zonal wind anomalies to stationary wave anomalies at 500 hPa in the Northern Hemisphere is similar to that observed by *Ting et al.* [1996].

## 5. Discussion

The composite difference in synoptic and stationary wave activity is much greater in the Atlantic than the Pacific (Fig. 3, right column). This difference appears consistent with the stronger NAM variation in the North Atlantic (Fig. 1). The pronounced zonal asymmetry over the North Atlantic during the high NAM phase is associated with the intensification of the climatological winter stationary wave pattern. The North Atlantic jet structure in the high NAM phase (see Fig. 3, bottom left) has stronger westerlies extending well into Norway and exhibits more Southwest-Northeast tilt than climatology. Similar intensification of the stationary waves has been noted in an observational context by *DeWeaver and Nigam* [1999].

Synoptic wave activity generation is likewise much stronger in the high NAM phase, as evidenced by the stronger vertical component of the **E** vectors. The exaggerated zonal asymmetry and extended protrusion of the North Atlantic jet appear to induce stronger and more localized baroclinically unstable zones poleward of 50°N. During the high NAM phase, anomalously cold conditions over the Labrador Sea and mild temperatures in the 35°-45° belt are reinforced by the NAM related stationary wave anomalies [*Wallace, J. M.*, personal communication]. As the modified stationary wave serves as the background flow for the synoptic waves, the intensified storm activity over the North Atlantic deviates further poleward from its climatological position. Indeed, observations of *Lau* [1988] document that the leading low frequency mode of the storm track variation in the North Atlantic is characterized by its meridional migration about the time-mean position.

**Acknowledgments.** This research was supported by the NOAA GFDL-Universities Consortium grant (Joint Institute for the Study of the Atmosphere and Ocean contribution number 673). The authors thank Dr. J. M. Wallace and D. W. J. Thompson for helpful discussions as well as Mary Jo Nath and Marc Michelsen for their computing assistance.

## References

DeWeaver, E. and S. Nigam, 1999: Do stationary waves drive the zonal-mean jet anomalies of the northern winter? submitted to *J. Climate.*

Feldstein, S. and S. Lee, 1996: Mechanisms of zonal index variability in an aquaplanet GCM, *J. Atmos. Sci.*, *53*, 3541-3555.

Hartmann, D. L. and F. Lo, 1998: Wave-driven zonal flow vacillation in the Southern Hemisphere, *J. Atmos. Sci.*, *55*, 1303-1315.

Hoskins, B. J., I. N. James, and G. H. White, 1983: The shape, propagation and mean-flow interaction of large-scale weather systems, *J. Atmos. Sci.*, *40*, 1595-1612.

James, I. N., 1994: *Introduction to Circulating Atmospheres*, 422 pp., University Press, Cambridge, England.

Lau, N.-C., 1988: Variability of the observed midlatitude storm tracks in relation to low-frequency changes in the circulation pattern, *J. Atmos. Sci.*, *45*, 2718-2743.

Lau, N.-C. and M. J. Nath, 1990: A general circulation model study of the atmospheric response to extratropical SST anomalies observed in 1950-79, *J. Climate.*, *3*, 965-989.

Limpasuvan, V. and D. L. Hartmann, 1999: Wave-maintained annular modes of climate variability, submitted to *J. Climate.*

North, G. R. and co-authors, 1982: Sampling errors in the estimation of empirical orthogonal functions, *Mon. Wea. Rev.*, *110*, 699-706.

Plumb, R. A., 1985: On the three-dimensional propagation of stationary waves, *J. Atmos. Sci.*, *42*, 217-229.

Robinson, W. A., 1991: The dynamics of the zonal index in a simple model of the atmosphere, *Tellus*, *43A*, 295-305.

Thompson, D. W. J. and J. M. Wallace, 1998: The Arctic oscillation signature in the wintertime geopotential height and temperature fields, *Geophys. Res. Lett.*, *25*, 1297-1300.

Thompson, D. W. J. and J. M. Wallace, 1999: Annular modes in the extratropical circulation, Part I: Month-to-month variability, to appear in *J. Climate.*

Ting, M. and co-authors, 1996: Northern hemisphere teleconnection patterns during extreme phases of the zonal-mean circulation, *J. Climate*, *9*, 2614-2633.

Yu, J.-Y. and D. L. Hartmann, 1993: Zonal flow vacillation and eddy forcing in a simple GCM of the atmosphere, *J. Atmos. Sci.*, *50*, 3244-3259.

V. Limpasuvan & D. L. Hartmann, University of Washington, Box 351640, Seattle, WA 98195. (e-mail: var@atmos.washington.edu; dennis@atmos.washington.edu)

(Received March 23, 1999; revised May 13, 1999;
accepted June 28, 1999.)